

Phosphorylation of PBX2, a novel downstream target of mTORC1, is determined by GSK3 and PP1

和田, 玲緒名

<https://hdl.handle.net/2324/6787497>

出版情報 : Kyushu University, 2022, 博士 (医学), 課程博士

バージョン :

権利関係 : Public access to the fulltext file is restricted for unavoidable reason (2)

1 Regular Paper/Biochemistry

2

3 **Phosphorylation of PBX2, a novel downstream target**
4 **of mTORC1, is determined by GSK3 and PP1**

5

6 Reona Wada¹, Shun Fujinuma¹, Hirokazu Nakatsumi¹, Masaki Matsumoto^{1,2} and
7 Keiichi I. Nakayama^{1*}

8

9 ¹Department of Molecular and Cellular Biology, Medical Institute of Bioregulation,
10 Kyushu University, 3-1-1 Maidashi, Higashi-ku, Fukuoka, Fukuoka 812-8582, Japan

11 ²Department of Omics and Systems Biology, Graduate School of Medical and Dental
12 Sciences, Niigata University, 757 Ichibancho, Asahimachi-dori, Chuo-ku, Niigata City,
13 Niigata 951-8510, Japan

14

15 *Correspondence: Keiichi I. Nakayama, Department of Molecular and Cellular Biology,
16 Medical Institute of Bioregulation, Kyushu University, 3-1-1 Maidashi, Higashi-ku,
17 Fukuoka, Fukuoka 812-8582, Japan. Tel.:+81-92-642-6815. Fax: +81-92-642-6819.

18 Email: nakayak1@bioreg.kyushu-u.ac.jp

19

20 Running head: Indirect PBX2 dephosphorylation by mTORC1

21

22 *Abbreviations:* DAPI, 4',6-diamidino-2-phenylindole; DMSO, dimethyl sulfoxide;
23 ERK, extracellular signal-regulated kinase; FOXK1, forkhead box K1; GSK3, glycogen
24 synthase kinase 3; HA, hemagglutinin; LARP1, La-related protein 1; MEK, ERK
25 kinase; mTORC1, mechanistic target of rapamycin complex 1; PBS, phosphate-buffered
26 saline; PBX2, pre-B cell leukemia transcription factor 2; **PI3K, phosphoinositide 3-**
27 **kinase; PDK1, phosphoinositide-dependent protein kinase 1; PP1, protein phosphatase**
28 **1; PP2A, protein phosphatase 2A; RAG, RAS-related GTP-binding protein; RHEB, Ras**
29 **homolog enriched in Brain; shRNA, short hairpin RNA; siRNA, small interfering RNA;**
30 **TBC1D7, TBC1 (TRE2-BUB2- CDC16) domain family member 7; TSC2, tuberous**
31 **sclerosis complex 2; WT, wild-type.**

32 **Summary**

33 **Mechanistic target of rapamycin complex 1 (mTORC1) is a serine-threonine**
34 **kinase that is activated by extracellular signals such as nutrients and growth**
35 **factors. It plays a key role in the control of various biological processes such as**
36 **protein synthesis and energy metabolism by mediating or regulating the**
37 **phosphorylation of multiple target molecules, some of which remain to be**
38 **identified. We have here reanalyzed a large-scale phosphoproteomics data set for**
39 **mTORC1 target molecules and identified pre-B cell leukemia transcription factor**
40 **2 (PBX2) as such a novel target that is dephosphorylated downstream of**
41 **mTORC1. We confirmed that PBX2, but not other members of the PBX family, is**
42 **dephosphorylated in an mTORC1 activity-dependent manner. Furthermore,**
43 **pharmacological and gene knockdown experiments revealed that glycogen**
44 **synthase kinase 3 (GSK3) and protein phosphatase 1 (PP1) are responsible for the**
45 **phosphorylation and dephosphorylation of PBX2, respectively. Our results thus**
46 **suggest that the balance between the antagonistic actions of GSK3 and PP1**
47 **determines the phosphorylation status of PBX2 and its regulation by mTORC1.**

48

49 *Keywords:* glycogen synthase kinase 3 (GSK3); mechanistic target of rapamycin
50 complex 1 (mTORC1); pre-B cell leukemia transcription factor 2 (PBX2);
51 phosphorylation; protein phosphatase 1 (PP1).

52

53 Mechanistic target of rapamycin complex 1 (mTORC1) is a serine-threonine kinase that
54 regulates cellular responses to nutrient-related signals such as insulin and amino acids
55 (1-3). Such signals activate mTORC1 on the cytoplasmic side of the lysosomal
56 membrane (1,2,4), and the activated complex subsequently phosphorylates a variety of
57 substrates, many of which regulate protein synthesis, autophagy, or metabolism to
58 promote cell growth (1-3). Rapamycin, an inhibitor of mTORC1, has effects on cancer,
59 immunity, and longevity (5-7), with these effects being largely dependent on attenuation
60 of the mTORC1-mediated phosphorylation of downstream molecules. In addition to its
61 classical function as a direct mediator of protein phosphorylation, recent studies
62 including phosphoproteomics analyses have shown that mTORC1 also promotes
63 dephosphorylation of downstream molecules in an indirect manner (8-11). We
64 previously showed that dephosphorylation of the transcription factor FOXK1 (forkhead
65 box K1) is regulated by mTORC1 and results in transcriptional activation of the gene
66 for C-C chemokine ligand 2 (CCL2), an inflammatory chemokine that triggers the
67 accumulation of monocytes and macrophages at sites of inflammation and thereby
68 promotes tumor growth (9). Although mTORC1 plays a key regulatory role in various
69 biological processes, many of its substrates remain to be identified, which has limited
70 overall understanding of such regulation. The identification of novel targets of
71 mTORC1 and elucidation of their mechanisms of action are expected to provide insight
72 into complex molecular pathways subject to regulation by this kinase.

73 In the present study, we have reanalyzed our previously reported
74 phosphoproteomics data obtained in a large-scale search for mTORC1 target molecules
75 (9) and have identified pre-B cell leukemia transcription factor 2 (PBX2) as such a
76 novel target. PBX proteins are transcription factors that belong to the highly conserved
77 TALE (three amino acid loop extension) family, with four paralogs (PBX1, PBX2,
78 PBX3, and PBX4) having been identified in human and mouse. PBX2 is expressed in a
79 variety of tissues and is thought to regulate the expression of many genes as a
80 homeobox cofactor that contributes to the control of development and cell
81 differentiation (12-14). PBX2 is also highly expressed in many cancer types, with such
82 high expression being associated with poor prognosis, especially in gastric cancer,
83 esophageal squamous cell carcinoma, non-small cell lung cancer, and gingival
84 squamous cell carcinoma (15-17). Indeed, depletion of PBX2 in gastric and esophageal
85 squamous cell carcinoma cell lines was found to inhibit colony formation *in vitro* and

86 tumorigenicity *in vivo* (16). In gastric cancer, PBX2 interacts with homeobox A6
87 (HOXA6), which plays an important role in cancer growth and metastasis, with this
88 interaction resulting in mutual protein stabilization and promotion of cancer migration
89 and invasion (14). Given that mTORC1 is also abnormally activated in these cancer
90 types and plays an important role in the proliferation and survival of the tumor cells
91 (3,6,18-22), mTORC1-mediated regulation of PBX2 phosphorylation might contribute
92 to their pathogenesis. The direct or indirect interaction between mTORC1 and PBX2
93 and the regulation of PBX2 phosphorylation state have not been investigated, however.

94 We now show that the phosphorylation state of PBX2 is dependent on
95 mTORC1 activity, and that Ser³³⁰ of the mouse and human proteins is the target site for
96 such phosphorylation. In contrast to a conventional target of mTORC1 action as a
97 kinase, PBX2 was found to be dephosphorylated in response to mTORC1 activation.
98 **Pharmacological and gene knockdown experiments revealed that phosphorylation of**
99 **PBX2 is indirectly regulated by mTORC1 and that glycogen synthase kinase 3 (GSK3)**
100 **and protein phosphatase 1 (PP1) are responsible for PBX2 phosphorylation and**
101 **dephosphorylation, respectively.** Our results thus suggest that GSK3 and PP1
102 antagonistically regulate PBX2 phosphorylation downstream of mTORC1.

103

104 **Materials and Methods**

105 ***Antibodies, reagents, and cell culture***

106 Antibodies for immunoblot analysis included those to the catalytic subunits of PP1
107 (clone E-9 monoclonal) obtained from Santa Cruz Biotechnology; those to PBX2
108 (polyclonal) from Atlas Antibodies; those to HSP90 (polyclonal) from Enzo Life
109 Sciences; those to p70 S6 kinase (clone 49D7), to phospho-p70 S6 kinase (clone 108D2
110 monoclonal), to 4E-BP1 (clone 53H11 monoclonal), to phospho-4E-BP1 (polyclonal),
111 to S6 (clone 5G10 monoclonal), to phospho-S6 (polyclonal), to GSK3 α/β (clone
112 D75D3 monoclonal), to AKT (polyclonal), to phospho-AKT (clone D9E monoclonal),
113 to ERK1/2 (polyclonal), to phospho-ERK1/2 (polyclonal), to MAPKAPK-2
114 (polyclonal), to phospho-MAPKAPK-2 (clone 27B7 monoclonal), and to the catalytic
115 subunits of PP2A (clone 52F8 monoclonal) from Cell Signaling Technology; and those
116 to the HA.11 epitope tag (clone 16B12 monoclonal) from BioLegend.
117 Immunocytofluorescence analysis was performed with the same antibodies to GSK3 α/β
118 and to the catalytic subunits of PP1 as well as with antibodies to the hemagglutinin

119 (HA) epitope tag (clone C29F4 monoclonal) obtained from Cell Signaling Technology.
120 Rapamycin was obtained from LC Laboratories; Torin 1 and Go6983 from Tocris
121 Bioscience; calyculin A from Cell Signaling Technology; LY294002, AZD6244,
122 SB203580, and SB216763 from Selleck Chemical; AktVIII from Sigma-Aldrich;
123 staurosporine from Wako Pure Chemical Industries; and CHIR99021 from Axon. 3T3-
124 L1 and HeLa cells were checked for mycoplasma contamination with the use of
125 MycoAlert (Lonza), and they were cultured under an atmosphere of 5% CO₂ at 37°C in
126 Dulbecco's modified Eagle's medium (DMEM) supplemented with 10% fetal bovine
127 serum, 1 mM sodium pyruvate, 2 mM L-glutamine, nonessential amino acids (10 ml/l,
128 Invitrogen), 2-mercaptoethanol (50 μM), and antibiotics. The cells were maintained in
129 medium containing a reduced serum concentration of 0.1% for 16 h before stimulation
130 with 100 nM insulin.

131

132 ***Retrovirus expression system***

133 Complementary DNAs encoding mouse PBX1, PBX2, PBX3, or PBX4, each with a
134 COOH-terminal HA epitope tag, were subcloned into pMX-puro (kindly provided by T.
135 Kitamura, The University of Tokyo, Japan) with the use of a NEBuilder HiFi DNA
136 Assembly system (New England Biolabs). The resulting vectors were introduced into
137 Plat-E packaging cells by transfection in order to generate recombinant retroviruses.
138 3T3-L1 cells were infected with the retroviruses in the presence of polybrene (5 μg/ml)
139 and were then cultured in the presence of puromycin (5 μg/ml) for selection.

140

141 ***RNA interference***

142 Small interfering RNAs (siRNAs) specific for human PP1 catalytic subunits A (s10930),
143 B (s10933), or C (s719) or for PP2A catalytic subunits A (s10957) or B (s10960), as
144 well as Silencer Select Negative Control #1 as a control, were obtained from Thermo
145 Fisher Scientific. Cells were transfected with the siRNAs with the use of Lipofectamine
146 RNAiMAX (Invitrogen). A retroviral vector (pCX4/Hygromycin) for expression of
147 short hairpin RNAs (shRNAs) was described previously (23), and 3T3-L1 cells were
148 depleted of GSK3α and GSK3β with the use of a modified shRNA (miR-E) system. The
149 target sequences were 5'-ACCCTTGGACAAAGGTGTTCAA-3' (nucleotides 1276–
150 1297) for mouse GSK3α, 5'-ACCGATCTGTCTTGAAGAAATA-3' (nucleotides 1312–
151 1333) for mouse GSK3β, and 5'-ACCGCCTGAAGTCTCTGATTAA-3' (nucleotides

152 1309–1330) for firefly luciferase as a control. The shRNA vectors were introduced into
153 Plat-E cells for generation of recombinant retroviruses, and 3T3-L1 cells were infected
154 with the retroviruses in the presence of polybrene (5 µg/ml) and were then cultured in
155 the presence of hygromycin B (300 µg/ml) for selection.

156

157 ***Immunoblot analysis***

158 Cells were washed with ice-cold phosphate-buffered saline (PBS), lysed in a lysis buffer
159 [50 mM Tris-HCl (pH 7.5), 150 mM NaCl, 0.5% Triton X-100, 4 mM sodium
160 orthovanadate, 4 mM EDTA, 100 mM NaF, 100 mM sodium pyrophosphate, 1 mM
161 phenylmethylsulfonyl fluoride, protease inhibitor cocktail (Complete, Roche)], and
162 fractionated by SDS-PAGE on a 10% gel or on an 8% gel supplemented with 50 µM
163 Phos-tag (NARD Institute) and 10 µM MnCl₂. Divalent cations were removed from
164 Phos-tag gels after electrophoresis by incubation twice for 5 min with transfer buffer
165 containing 1 mM EDTA.

166

167 ***Immunofluorescence analysis***

168 Cells were fixed for 10 min with 4% paraformaldehyde in PBS, washed three times
169 with PBS, and incubated overnight at 4°C in staining buffer [0.45% Triton X-100 and
170 1% BSA fraction V (Roche) in PBS] containing primary antibodies. They were then
171 washed three times with PBS before incubation for 30 min at room temperature with
172 Alexa Fluor 488–conjugated secondary antibodies (Invitrogen) in staining buffer.
173 Nuclei were stained with 4',6-diamidino-2-phenylindole (DAPI). The cells were
174 examined with a laser-scanning confocal microscope (LSM700, Carl Zeiss, or BZ-
175 X800, Keyence).

176

177 ***Statistical analysis***

178 Quantitative data are presented as means ± SEM and were analyzed with Dunnett's test
179 as performed with Rstudio software. A *P* value of <0.05 was considered statistically
180 significant.

181

182 **Results**

183 ***Identification of PBX2 as a downstream effector of mTORC1***

184 To identify new targets of mTORC1 that are dephosphorylated in response to mTORC1

185 activation, we first reanalyzed large-scale phosphoproteomics data obtained in our
186 previous study (9) for HeLa cells subjected to various conditions that activate mTORC1
187 including stimulation with serum, insulin, or amino acids (Fig. 1A). A total of 75
188 proteins was found to be dephosphorylated in response to serum stimulation in a
189 manner sensitive to rapamycin but not to U0126, an inhibitor of the extracellular signal-
190 regulated kinase (ERK) kinase MEK. In addition, 1480 and 319 proteins were
191 dephosphorylated in response to insulin or amino acid stimulation, respectively, in a
192 time-dependent manner. Eleven of these various proteins were commonly
193 dephosphorylated under all three conditions, and among these proteins only PBX2,
194 FOXK1, and La-related protein 1 (LARP1) underwent dephosphorylation at the same
195 sites under all three conditions (Fig. 1B). Given that FOXK1 (9,11,24,25) and LARP1
196 (26) were already known to be regulated downstream of mTORC1, we focused on the
197 mechanism underlying regulation of the phosphorylation of PBX2, which had not been
198 previously identified as a downstream effector of mTORC1, in the present study.

199

200 ***mTORC1-dependent dephosphorylation of PBX2***

201 We next performed Phos-tag SDS-PAGE to detect changes in the phosphorylation state
202 of PBX2. In this approach, the interaction of the phosphate groups of phosphorylated
203 proteins with Phos-tag slows protein migration rate, allowing the separation of
204 phosphorylated and nonphosphorylated forms of a given protein without the use of
205 phospho-specific antibodies (27). Immunoblot analysis after Phos-tag SDS-PAGE
206 revealed that the electrophoretic mobility of the immunoreactive band corresponding to
207 PBX2 was increased in response to insulin stimulation in 3T3-L1 cells (Fig. 2A),
208 suggestive of PBX2 dephosphorylation. This mobility shift was greatly attenuated by
209 treatment of the cells with the mTORC1 inhibitors rapamycin or Torin 1, indicative of
210 its dependence on mTORC1 activation. Furthermore, only PBX2 among the four
211 paralogs of the PBX family showed a change in electrophoretic mobility in response to
212 mTORC1 activation (Fig. 2B). These results thus suggested that PBX2 is a novel target
213 for mTORC1 activity-dependent dephosphorylation.

214

215 ***Ser³³⁰ of PBX2 is dephosphorylated in the nucleus***

216 Our phosphoproteomics analysis revealed that Ser³³⁰ of PBX2 was dephosphorylated in
217 an mTORC1-dependent manner (Fig. 1B). To validate this result biochemically, we

218 generated 3T3-L1 cells expressing a mutant (S330A) of PBX2 in which Ser³³⁰ is
219 replaced by Ala and which mimics the Ser³³⁰-dephosphorylated form of the protein.
220 Phos-tag SDS-PAGE and immunoblot analysis revealed that the electrophoretic
221 mobility of the S330A mutant was not affected by the activation state of mTORC1 and
222 was similar to that of wild-type (WT) PBX2 in cells stimulated with insulin (Fig. 3A),
223 consistent with the notion that Ser³³⁰ of PBX2 is dephosphorylated in response to
224 mTORC1 activation. We also generated 3T3-L1 cells expressing mutants (S330D and
225 S330E) of PBX2 in which Ser³³⁰ is replaced by Asp or Glu and which mimic the Ser³³⁰-
226 phosphorylated form of the protein. Phos-tag SDS-PAGE and immunoblot analysis
227 revealed that the electrophoretic mobility of the S330D mutant was also not affected by
228 mTORC1 activation status and was similar to that of the S330A mutant, suggesting that
229 Asp did not interact with Phos-tag.

230 PBX2 and mTORC1 differ in their subcellular localizations, with the former
231 localizing predominantly to the nucleus (28) and the latter to the cytoplasm (29). Given
232 that PBX2 is dephosphorylated in an mTORC1-dependent manner, we examined
233 whether its subcellular localization might be dependent on its phosphorylation state.
234 However, immunocytofluorescence staining revealed that WT and S330A, S330D, and
235 S330E mutant forms of PBX2 were all localized to the nucleus in 3T3-L1 cells (Fig.
236 3B). Consistent with this observation, the subcellular localization of PBX2(WT) was
237 not affected by treatment of cells with rapamycin, Torin 1, or insulin (Fig. 3C and D),
238 suggesting that PBX2 localizes to the nucleus regardless of the phosphorylation state of
239 Ser³³⁰. Together, our results thus indicated that PBX2 dephosphorylation occurs in the
240 nucleus as a result of an indirect action of mTORC1, and that signaling between
241 mTORC1 in the cytoplasm and PBX2 in the nucleus may be mediated by some
242 unidentified factor.

243

244 ***mTORC1 regulates PBX2 phosphorylation through GSK3***

245 Our finding that Ser³³⁰ of PBX2 is phosphorylated in cells in which mTORC1 is
246 inactive suggested the presence of another kinase that phosphorylates PBX2. To
247 identify such a kinase, we examined the effects of various kinase inhibitors on the
248 phosphorylation of PBX2 at Ser³³⁰ in 3T3-L1 cells exposed to both insulin and Torin 1.
249 Treatment of the cells with staurosporine, a broad-spectrum kinase inhibitor, attenuated
250 the signal intensity of the band corresponding to Ser³³⁰-phosphorylated PBX2 and

251 increased that of the band corresponding to the Ser³³⁰-dephosphorylated protein in a
252 concentration-dependent manner (Fig. 4A). On the other hand, inhibitors of
253 phosphatidylinositol 3-kinase (LY294002) and AKT (AktVIII), both of which function
254 upstream of mTORC1, had no effect on the phosphorylation state of PBX2. Given that
255 insulin-stimulated phosphorylation of Ser⁴⁷³ of AKT was shown to be mediated by
256 mTORC2 (30), Torin 1 treatment inhibited the phosphorylation of Ser⁴⁷³ of AKT. We
257 also found that a protein kinase C inhibitor (Go6983) partially inhibited Ser³³⁰-
258 phosphorylation of PBX2, whereas inhibitors of MEK (AZD6244) and p38 mitogen-
259 activated protein kinase (SB203580) had no effect on PBX2 phosphorylation status
260 (Fig. 4B). In contrast, inhibitors of GSK3 (SB216763 and CHIR99021) were found to
261 reduce the signal intensity of the band corresponding to Ser³³⁰-phosphorylated PBX2
262 and to increase that of the band corresponding to the Ser³³⁰-dephosphorylated protein in
263 a concentration-dependent manner (Fig. 4B and C). Consistent with these results,
264 shRNA-mediated depletion of GSK3 α or GSK3 β in 3T3-L1 cells attenuated the
265 phosphorylation of PBX2 at Ser³³⁰, and this effect was more pronounced in cells
266 depleted of both GSK3 α and GSK3 β (Fig. 4C).

267 Given that inhibition of mTORC1 has been shown to result in the nuclear
268 accumulation of GSK3 and consequent phosphorylation by GSK3 of its substrates in the
269 nucleus (24), we performed immunocytofluorescence staining to examine the
270 subcellular localization of GSK3 in serum-deprived 3T3-L1 cells exposed to insulin
271 with or without rapamycin or Torin 1. Activation of mTORC1 by insulin stimulation
272 was associated with translocation of GSK3 from the nucleus to the cytoplasm, whereas
273 inhibition of mTORC1 activity by rapamycin or Torin 1 attenuated this effect (Fig. 4D).
274 Overall, these results suggested that mTORC1 regulates the nuclear-cytoplasmic
275 translocation of GSK3, and that suppression of mTORC1 activity promotes the nuclear
276 accumulation of GSK3 and consequent phosphorylation of PBX2 at Ser³³⁰.

277

278 **PP1 dephosphorylates PBX2 at Ser³³⁰**

279 To identify intervening molecules that mediate dephosphorylation of PBX2 in response
280 to mTORC1 activation, we examined several candidate phosphatases. Given that the
281 serine-threonine protein phosphatases PP1 and PP2A are responsible for >90% of
282 protein phosphatase activity in eukaryotic cells (31), we focused on these enzymes and
283 examined whether calyculin A, which inhibits the activity of both PP1 and PP2A, might

284 suppress mTORC1-dependent PBX2 dephosphorylation. Treatment of serum-deprived
285 3T3-L1 cells with calyculin A inhibited in a concentration-dependent manner the change
286 in the electrophoretic mobility of PBX2 induced by insulin stimulation (Fig. 5A). We
287 also found that siRNA-mediated depletion of the catalytic subunits of PP1 in HeLa cells
288 increased the signal intensity of the band corresponding to Ser³³⁰-phosphorylated PBX2
289 relative to that of the band corresponding to the Ser³³⁰-dephosphorylated protein under
290 both basal and insulin-stimulated conditions (Fig. 5B and C). In contrast, depletion of
291 the catalytic subunits of PP2A did not affect the signal intensity of the bands
292 corresponding to Ser³³⁰-phosphorylated or Ser³³⁰-dephosphorylated PBX2 in the
293 absence or presence of insulin stimulation (Fig. 5B and C), suggesting that PP2A may
294 not contribute to PBX2 dephosphorylation at this site. **In addition, depletion of the
295 catalytic subunits of PP2A resulted in an increase in the signal intensity of a band with
296 the highest mobility shift, which likely represents a hyper-dephosphorylated form of
297 PBX2. Although the mechanism underlying this phenomenon is unclear, one possible
298 explanation is that the depletion of the catalytic subunits of PP2A might result in up-
299 regulation of activity or expression level of the other protein phosphatases such as PP1
300 that target PBX2, through an unknown compensatory mechanism. Another possibility is
301 that PP2A activates some kinases that phosphorylate PBX2, and that the depletion of the
302 catalytic subunits of PP2A might result in inactivation of such kinases, leading to an
303 increase in the amount of non-phosphorylated forms of PBX2. Given the difference in
304 mobility of the bands, phosphorylation of PBX2 likely occurs at multiple residues other
305 than Ser³³⁰. Dephosphorylation of PBX2 at Ser³³⁰ was also observed under conditions of
306 simultaneous inhibition of GSK3 and mTORC1 (Fig. 4A and C), suggesting that PP1
307 might mediate dephosphorylation of PBX2 at Ser³³⁰ in an mTORC1 activity-
308 independent manner.**

309 The catalytic subunits of PP1 show a broad tissue and subcellular distribution,
310 with their subcellular localization being dynamically altered by interaction with various
311 proteins (31,32). We found that the catalytic subunits of PP1 were localized to the
312 nucleus of 3T3-L1 cells both under the basal condition and after stimulation with
313 insulin in the absence or presence of rapamycin or Torin 1 (Fig. 5D). These results thus
314 suggested that the subcellular localization of PP1 is independent of insulin stimulation
315 and thus of mTORC1 activity in these cells.

316

317 **Discussion**

318 We have here shown that PBX2 undergoes dephosphorylation at Ser³³⁰ in an mTORC1
319 activity-dependent manner, consistent with the reanalysis of our phosphoproteomics
320 data implicating PBX2 as a novel target molecule for mTORC1. Furthermore,
321 immunofluorescence staining of cells expressing phosphomimetic or dephosphomimetic
322 Ser³³⁰ mutants of PBX2 revealed that PBX2 localizes to the nucleus regardless of its
323 phosphorylation state. Consistent with this finding, we also showed that PBX2(WT)
324 localizes to the nucleus independently of mTORC1 activity. Our results thus suggest
325 that phosphorylation of PBX2 is regulated in the nucleus.

326 The serine-threonine kinase GSK3 has two paralogs, GSK3 α and GSK3 β , in
327 mammals and is known to phosphorylate >100 substrates important for the regulation of
328 cell growth and metabolism. The activity of GSK3 α is regulated predominantly by
329 phosphorylation at Ser²¹ (inhibiting) and Tyr²⁷⁹ (activating), with Ser⁹ and Tyr²¹⁶ being
330 the corresponding residues targeted for regulation in GSK3 β . GSK3 is active in cells
331 under basal conditions and is inactivated by inhibitory phosphorylation in response to
332 cell stimulation by hormones or growth factors (33). Furthermore, mTORC1 inhibition
333 by rapamycin treatment has been shown to promote redistribution of GSK3 from the
334 cytoplasm to the nucleus and thereby to affect phosphorylation of GSK3 substrates, **but**
335 **it did not alter the phosphorylation state of Ser²¹ of GSK3 α and Ser⁹ of GSK3 β (24,34).**
336 **This scenario is consistent with our experimental results showing that phosphorylation**
337 **of PBX2 at Ser³³⁰ is mediated by GSK3 that accumulates in the nucleus in cells in**
338 **which mTORC1 is inactive. Similarly, the phosphorylation state of GSK3 might not be**
339 **affected by mTORC1 activation as was the case for previous studies.**

340 Protein serine-threonine phosphatases PP1 and PP2A generally form
341 holoenzymes consisting of multiple functionally distinct subunits. In particular, the
342 regulatory subunits have been shown to determine the catalytic activity, substrate
343 specificity and subcellular localization of such phosphatases (35,36). Given that both
344 PP1 and PP2A contain catalytic and regulatory subunits, the latter likely regulates their
345 binding specificity to the substrates including PBX2. PP1 regulates diverse cellular
346 processes through substrate dephosphorylation and is composed of a catalytic subunit
347 and a variety of regulatory subunits, with the interaction of these subunits having been
348 shown to control substrate specificity and localization of the holoenzyme (31,32). For
349 example, PPP1R3B, a regulatory subunit of PP1 that contributes to the regulation of

350 blood glucose clearance and glycogen synthesis in the liver, associates with and thereby
351 promotes the dephosphorylation of glycogen synthase in response to its own
352 phosphorylation by insulin-activated AKT (37). We found that PP1 mediated the
353 dephosphorylation of PBX2 at Ser³³⁰ and was localized to the nucleus of cells in a
354 manner independent of mTORC1 activity.

355 We have demonstrated in the present study that mTORC1 regulates the
356 phosphorylation state of PBX2 by controlling the subcellular localization of GSK3.
357 Given that insulin stimulation activates the PI3K-PDK1-AKT axis upstream of
358 mTORC1 (1,4), this pathway is possibly one of the key signals that regulate mTORC1-
359 GSK3-mediated PBX2 phosphorylation. On the other hand, as shown in a previous
360 study (37), it is also possible that the insulin-AKT axis directly regulates PP1
361 phosphatase activity in an mTORC1-GSK-independent manner. However, our results
362 have shown that insulin stimulation no longer affects the phosphorylation state of PBX2
363 at Ser³³⁰ in the context of complete GSK3 depletion, suggesting that the GSK3-
364 independent insulin-AKT-PP1 axis minimally contributes to the regulation of PBX2
365 phosphorylation state. Together with a number of supportive data showing that PBX2 is
366 dephosphorylated in an mTORC1 activation-dependent manner, we concluded that the
367 mTORC1-mediated regulation of GSK3 localization predominantly determines the
368 phosphorylation state of PBX2, downstream of nutrient-related signals such as insulin.

369 There are several limitations to our study. First, although we examined by
370 multiple approaches the roles of GSK3 and PP1 in PBX2 phosphorylation and
371 dephosphorylation, respectively, it remains possible that GSK3 and PP1 actually
372 regulate other downstream kinases and phosphatases that directly determine the
373 phosphorylation status of PBX2. Second, whereas 3T3-L1 cells (mouse) were used for
374 most experiments, HeLa cells (human) were used to examine the effects of PP1 and
375 PP2A depletion, given that 3T3-L1 cells manifested marked growth inhibition in
376 response to such depletion. On the other hand, our results indicate that mTORC1-
377 dependent regulation of PBX2 phosphorylation is conserved between these two species,
378 suggesting that it may play an important role *in vivo*.

379 Activation of mTORC1 regulates many biological processes including
380 translation, autophagy, metabolism, and cell proliferation, not only through direct
381 phosphorylation of key substrates but also through inhibition of the phosphorylation of
382 numerous other targets. Given that mTORC1 is abnormally activated in many cancer

383 types (3-6, 18-22) and PBX2 is highly expressed in many cancer types (15-17),
384 mTORC1 likely promotes the progression of these cancers by altering the stability of
385 PBX2 as a protein and transcriptional activities such as PBX2 DNA binding affinity and
386 binding ability to co-factors through the regulation of PBX2 phosphorylation status.
387 Such biological aspects of PBX2 phosphorylation regulation in normal as well as cancer
388 cell contexts await future study.

389

390 **Acknowledgements**

391 We thank T. Akagi for the pCX4 system; S. Mise, T. Higa, and other laboratory
392 members for discussion; as well as A. Ohta for help with preparation of the manuscript.

393

394 **Conflict of Interest Statement**

395 The authors have no conflicts of interest to declare.

396

397 **References**

- 398 1. Shimobayashi, M., and Hall, M. N. (2014) Making new contacts: the mTOR
399 network in metabolism and signalling crosstalk. *Nat. Rev. Mol. Cell Biol.* **15**, 155-
400 162
- 401 2. Liu, G. Y., and Sabatini, D. M. (2020) mTOR at the nexus of nutrition, growth,
402 ageing and disease. *Nat. Rev. Mol. Cell Biol.* **21**, 183-203
- 403 3. Cornu, M., Albert, V., and Hall, M. N. (2013) mTOR in aging, metabolism, and
404 cancer. *Curr Opin Genet Dev* **23**, 53-62
- 405 4. Gonzalez, A., and Hall, M. N. (2017) Nutrient sensing and TOR signaling in yeast
406 and mammals. *EMBO J.* **36**, 397-408
- 407 5. Lushchak, O., Strilbytska, O., Piskovatska, V., Storey, K. B., Koliada, A., and
408 Vaiserman, A. (2017) The role of the TOR pathway in mediating the link between
409 nutrition and longevity. *Mech. Ageing Dev.* **164**, 127-138
- 410 6. Li, J., Kim, S. G., and Blenis, J. (2014) Rapamycin: one drug, many effects. *Cell*
411 *Metab.* **19**, 373-379
- 412 7. Elloso, M. M., Azrolan, N., Sehgal, S. N., Hsu, P. L., Phiel, K. L., Kopec, C. A.,
413 Basso, M. D., and Adelman, S. J. (2003) Protective effect of the
414 immunosuppressant sirolimus against aortic atherosclerosis in apo E-deficient
415 mice. *Am. J. Transplant.* **3**, 562-569
- 416 8. Yu, Y., Yoon, S. O., Poulgiannis, G., Yang, Q., Ma, X. M., Villen, J., Kubica, N.,
417 Hoffman, G. R., Cantley, L. C., Gygi, S. P., and Blenis, J. (2011)
418 Phosphoproteomic analysis identifies Grb10 as an mTORC1 substrate that
419 negatively regulates insulin signaling. *Science* **332**, 1322-1326
- 420 9. Nakatsumi, H., Matsumoto, M., and Nakayama, K. I. (2017) Noncanonical
421 Pathway for Regulation of CCL2 Expression by an mTORC1-FOXK1 Axis
422 Promotes Recruitment of Tumor-Associated Macrophages. *Cell Rep.* **21**, 2471-
423 2486
- 424 10. Hsu, P. P., Kang, S. A., Rameseder, J., Zhang, Y., Ottina, K. A., Lim, D., Peterson,
425 T. R., Choi, Y., Gray, N. S., Yaffe, M. B., Marto, J. A., and Sabatini, D. M. (2011)
426 The mTOR-regulated phosphoproteome reveals a mechanism of mTORC1-
427 mediated inhibition of growth factor signaling. *Science* **332**, 1317-1322
- 428 11. He, L., Gomes, A. P., Wang, X., Yoon, S. O., Lee, G., Nagiec, M. J., Cho, S.,
429 Chavez, A., Islam, T., Yu, Y., Asara, J. M., Kim, B. Y., and Blenis, J. (2018)

- 430 mTORC1 Promotes Metabolic Reprogramming by the Suppression of GSK3-
431 Dependent Foxk1 Phosphorylation. *Mol. Cell* **70**, 949-960 e944
- 432 12. Moens, C. B., and Selleri, L. (2006) Hox cofactors in vertebrate development. *Dev.*
433 *Biol.* **291**, 193-206
- 434 13. Longobardi, E., Penkov, D., Mateos, D., De Florian, G., Torres, M., and Blasi, F.
435 (2014) Biochemistry of the tale transcription factors PREP, MEIS, and PBX in
436 vertebrates. *Dev. Dyn.* **243**, 59-75
- 437 14. Lin, J., Zhu, H., Hong, L., Tang, W., Wang, J., Hu, H., Wu, X., Chen, Y., Liu, G.,
438 Yang, Q., Li, J., Wang, Y., Lin, Z., Xiao, Y., Dai, W., Huang, M., Li, G., Li, A.,
439 Wang, J., Xiang, L., and Liu, S. (2021) Coexpression of HOXA6 and PBX2
440 promotes metastasis in gastric cancer. *Aging (Albany N. Y.)* **13**, 6606-6624
- 441 15. Qiu, Y., Morii, E., Tomita, Y., Zhang, B., Matsumura, A., Kitaichi, M., Okumura,
442 M., and Aozasa, K. (2009) Prognostic significance of pre B cell leukemia
443 transcription factor 2 (PBX2) expression in non-small cell lung carcinoma.
444 *Cancer Sci.* **100**, 1198-1209
- 445 16. Qiu, Y., Song, B., Zhao, G., Deng, B., Makino, T., Tomita, Y., Wang, J., Luo, W.,
446 Doki, Y., Aozasa, K., and Morii, E. (2010) Expression level of Pre B cell leukemia
447 homeobox 2 correlates with poor prognosis of gastric adenocarcinoma and
448 esophageal squamous cell carcinoma. *Int. J. Oncol.* **36**, 651-663
- 449 17. Qiu, Y., Wang, Z. L., Jin, S. Q., Pu, Y. F., Toyosawa, S., Aozasa, K., and Morii, E.
450 (2012) Expression level of pre-B-cell leukemia transcription factor 2 (PBX2) as a
451 prognostic marker for gingival squamous cell carcinoma. *J Zhejiang Univ Sci B*
452 **13**, 168-175
- 453 18. Harsha, C., Banik, K., Ang, H. L., Girisa, S., Vikkurthi, R., Parama, D., Rana, V.,
454 Shabnam, B., Khatoon, E., Kumar, A. P., and Kunnumakkara, A. B. (2020)
455 Targeting AKT/mTOR in Oral Cancer: Mechanisms and Advances in Clinical
456 Trials. *Int. J. Mol. Sci.* **21**
- 457 19. Hibdon, E. S., Razumilava, N., Keeley, T. M., Wong, G., Solanki, S., Shah, Y. M.,
458 and Samuelson, L. C. (2019) Notch and mTOR Signaling Pathways Promote
459 Human Gastric Cancer Cell Proliferation. *Neoplasia* **21**, 702-712
- 460 20. Shi, N., Yu, H., and Chen, T. (2019) Inhibition of esophageal cancer growth
461 through the suppression of PI3K/AKT/mTOR signaling pathway. *Onco Targets*
462 *Ther.* **12**, 7637-7647

- 463 21. Tan, A. C. (2020) Targeting the PI3K/Akt/mTOR pathway in non-small cell lung
464 cancer (NSCLC). *Thorac Cancer* **11**, 511-518
- 465 22. Tapia, O., Riquelme, I., Leal, P., Sandoval, A., Aedo, S., Weber, H., Letelier, P.,
466 Bellolio, E., Villaseca, M., Garcia, P., and Roa, J. C. (2014) The
467 PI3K/AKT/mTOR pathway is activated in gastric cancer with potential prognostic
468 and predictive significance. *Virchows Arch.* **465**, 25-33
- 469 23. Oshikawa, K., Matsumoto, M., Kodama, M., Shimizu, H., and Nakayama, K. I.
470 (2020) A fail-safe system to prevent oncogenesis by senescence is targeted by
471 SV40 small T antigen. *Oncogene* **39**, 2170-2186
- 472 24. He, L., Fei, D. L., Nagiec, M. J., Mutvei, A. P., Lamprakis, A., Kim, B. Y., and
473 Blenis, J. (2019) Regulation of GSK3 cellular location by FRAT modulates
474 mTORC1-dependent cell growth and sensitivity to rapamycin. *Proc. Natl. Acad.
475 Sci. U. S. A.* **116**, 19523-19529
- 476 25. Nakatsumi, H., Oka, T., Higa, T., Shirane, M., and Nakayama, K. I. (2018)
477 Nuclear-cytoplasmic shuttling protein PP2A(B56) contributes to mTORC1-
478 dependent dephosphorylation of FOXK1. *Genes Cells* **23**, 599-605
- 479 26. Berman, A. J., Thoreen, C. C., Dedeic, Z., Chettle, J., Roux, P. P., and Blagden, S.
480 P. (2021) Controversies around the function of LARP1. *RNA Biol.* **18**, 207-217
- 481 27. Kinoshita, E., Kinoshita-Kikuta, E., Takiyama, K., and Koike, T. (2006)
482 Phosphate-binding tag, a new tool to visualize phosphorylated proteins. *Mol Cell
483 Proteomics* **5**, 749-757
- 484 28. Ota, T., Asahina, H., Park, S. H., Huang, Q., Minegishi, T., Auersperg, N., and
485 Leung, P. C. (2008) HOX cofactors expression and regulation in the human ovary.
486 *Reprod. Biol. Endocrinol.* **6**, 49
- 487 29. Betz, C., and Hall, M. N. (2013) Where is mTOR and what is it doing there? *J.
488 Cell Biol.* **203**, 563-574
- 489 30. Oh, W. J., and Jacinto, E. (2011) mTOR complex 2 signaling and functions. *Cell
490 Cycle* **10**, 2305-2316
- 491 31. Rebelo, S., Santos, M., Martins, F., da Cruz e Silva, E. F., and da Cruz e Silva, O.
492 A. (2015) Protein phosphatase 1 is a key player in nuclear events. *Cell. Signal.* **27**,
493 2589-2598
- 494 32. Korrodi-Gregorio, L., Esteves, S. L., and Fardilha, M. (2014) Protein phosphatase
495 1 catalytic isoforms: specificity toward interacting proteins. *Transl. Res.* **164**, 366-

- 496 391
- 497 33. Evangelisti, C., Chiarini, F., Paganelli, F., Marmioli, S., and Martelli, A. M.
498 (2020) Crosstalks of GSK3 signaling with the mTOR network and effects on
499 targeted therapy of cancer. *Biochim Biophys Acta Mol Cell Res* **1867**, 118635
- 500 34. Bautista, S. J., Boras, I., Vissa, A., Mecica, N., Yip, C. M., Kim, P. K., and
501 Antonescu, C. N. (2018) mTOR complex 1 controls the nuclear localization and
502 function of glycogen synthase kinase 3beta. *J. Biol. Chem.* **293**, 14723-14739
- 503 35. Hoermann, B., and Kohn, M. (2021) Evolutionary crossroads of cell signaling:
504 PP1 and PP2A substrate sites in intrinsically disordered regions. *Biochem. Soc.*
505 *Trans.* **49**, 1065-1074
- 506 36. Brautigan, D. L., and Shenolikar, S. (2018) Protein Serine/Threonine
507 Phosphatases: Keys to Unlocking Regulators and Substrates. *Annu. Rev. Biochem.*
508 **87**, 921-964
- 509 37. Li, Q., Zhao, Q., Zhang, J., Zhou, L., Zhang, W., Chua, B., Chen, Y., Xu, L., and
510 Li, P. (2019) The Protein Phosphatase 1 Complex Is a Direct Target of AKT that
511 Links Insulin Signaling to Hepatic Glycogen Deposition. *Cell Rep.* **28**, 3406-3422
512 e3407
- 513

514 **Figure Legends**

515 **Fig. 1. Identification of PBX2 as a downstream effector of mTORC1.** (A) Scheme
516 for the acquisition of phosphoproteomics data in our previous study (9). Serum-
517 deprived HeLa cells were exposed to 10 nM rapamycin or 10 μ M U0126 for 30 min
518 before stimulation with serum for 20 min. Alternatively, HeLa cells were either
519 deprived of serum for 16 h before stimulation with insulin for the indicated times or
520 deprived of amino acids for 5 h before stimulation with amino acids for the indicated
521 times. (B) Venn diagram showing the overlap in proteins found to undergo
522 dephosphorylation in response to serum in a rapamycin-sensitive manner (but not in a
523 U0126-sensitive manner) or in response to insulin or amino acid stimulation in a time-
524 dependent manner (left panel). The overlap in the dephosphorylation sites for the 11
525 proteins found to be dephosphorylated under all three conditions is also shown (right
526 panel).

527

528 **Fig. 2. mTORC1-dependent dephosphorylation of PBX2.** (A) Serum-deprived 3T3-
529 L1 cells were incubated with 10 nM rapamycin, 100 nM Torin 1, or 0.1% dimethyl
530 sulfoxide (DMSO, vehicle) for 1 h and then in the additional presence of 100 nM
531 insulin for the indicated times, after which cell extracts were subjected to SDS-PAGE
532 with or without Phos-Tag followed by immunoblot (IB) analysis with antibodies to the
533 indicated total or phosphorylated (p-) proteins. Phosphorylation of p70 S6 kinase (S6K),
534 S6, and 4E-BP1 was examined to monitor mTORC1 activity. (B) Serum-deprived 3T3-
535 L1 cells infected with retroviruses encoding HA epitope-tagged PBX1, PBX2, PBX3,
536 or PBX4 were incubated with 10 nM rapamycin, 100 nM Torin 1, or 0.1% DMSO for 1
537 h and then in the additional absence or presence of 100 nM insulin for 30 min, after
538 which cell extracts were analyzed as in (A). HSP90 was examined as a loading control.

539

540 **Fig. 3. Ser³³⁰ of PBX2 is dephosphorylated in the nucleus in an mTORC1-**
541 **dependent manner.** (A) Serum-deprived 3T3-L1 cells infected with retroviruses
542 encoding HA epitope-tagged WT or mutant (S330A or S330D) forms of PBX2 were
543 incubated with 10 nM rapamycin or 100 nM Torin 1 for 1 h and then in the additional
544 absence or presence of 100 nM insulin for 30 min, after which cell extracts were
545 subjected to SDS-PAGE with or without Phos-tag followed by immunoblot analysis
546 with antibodies to the indicated proteins. (B–D) Immunocytofluorescence analysis of

547 the HA epitope (green) in 3T3-L1 cells expressing HA-tagged WT or mutant (S330A,
548 S330D, or S330E) forms of PBX2 (B), in 3T3-L1 cells expressing HA-PBX2(WT) and
549 incubated with or without 10 nM rapamycin or 100 nM Torin 1 for 1 h (C), or in 3T3-
550 L1 cells expressing HA-PBX2(WT) that were deprived of serum and then incubated
551 with 100 nM insulin for the indicated times (D). Nuclei were stained with DAPI (blue).
552 Scale bars, 10 μ m.

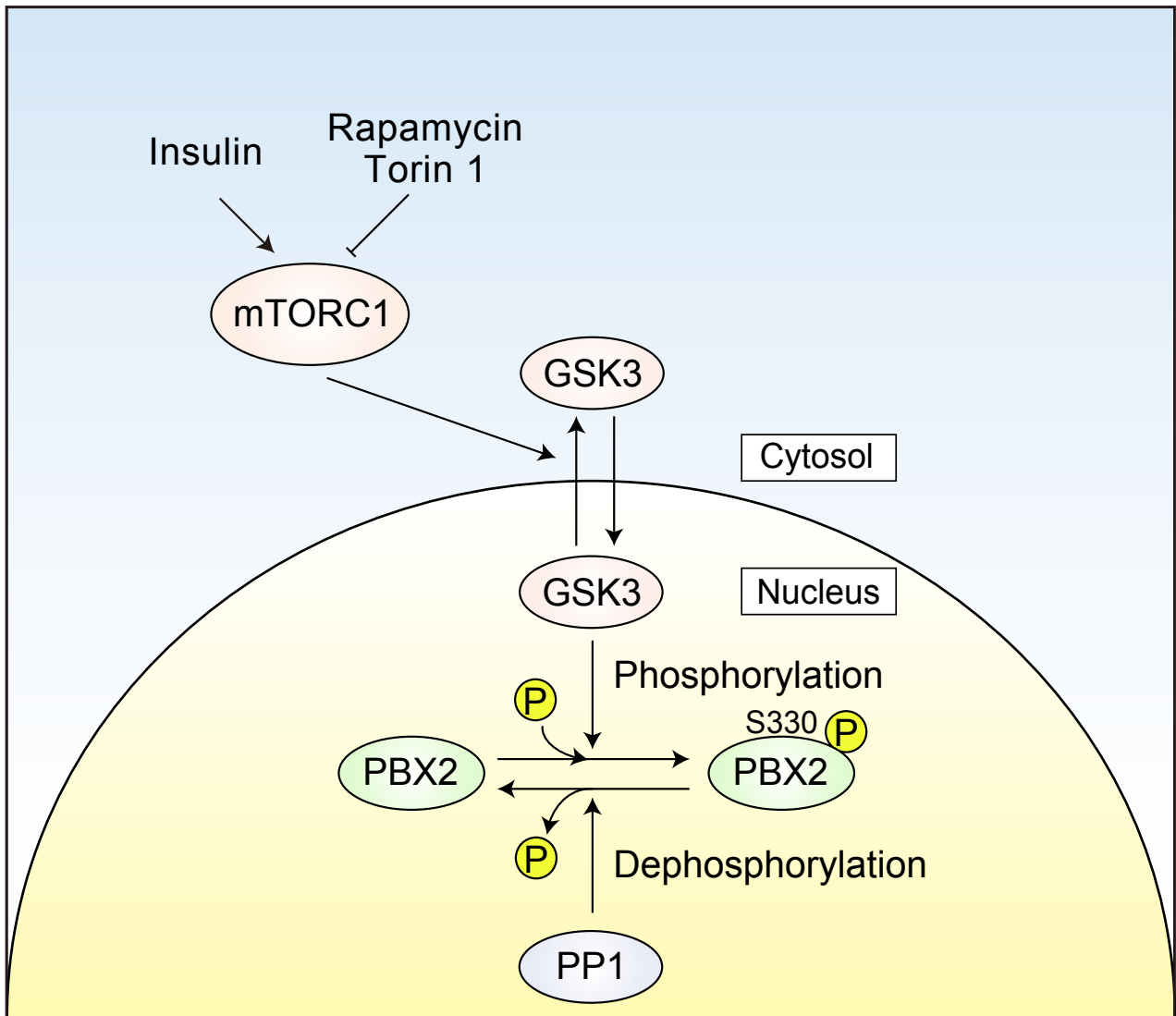
553

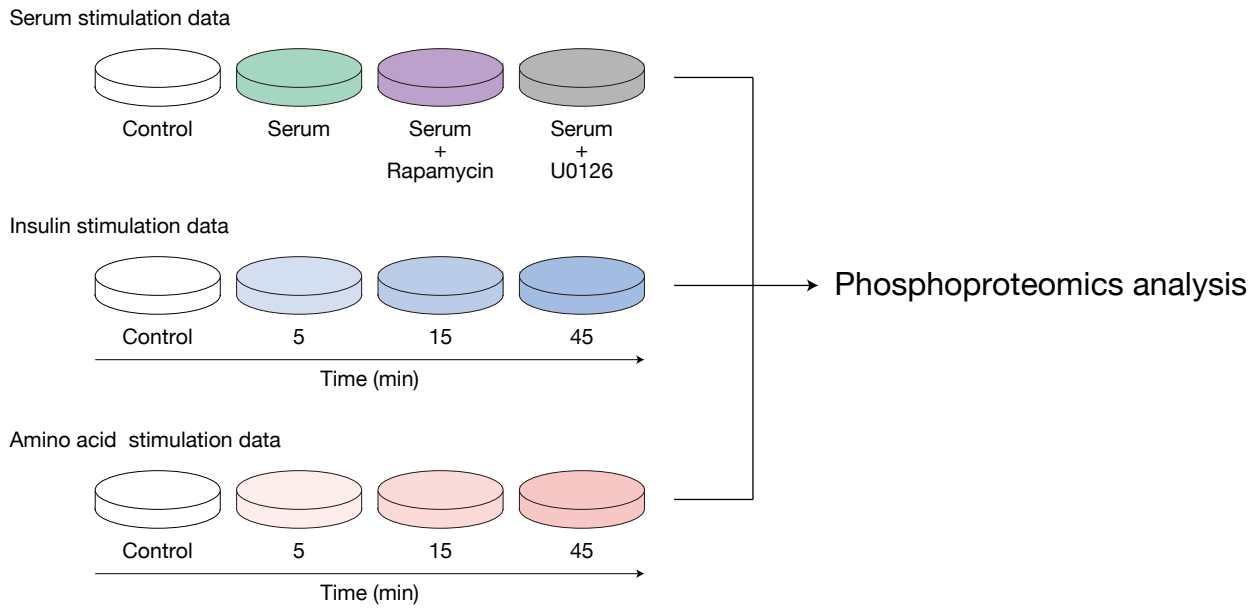
554 **Fig. 4. mTORC1 regulates PBX2 phosphorylation through GSK3.** (A and B) Serum-
555 deprived 3T3-L1 cells were incubated with various inhibitors [Torin1 (100 nM),
556 staurosporine (10, 100 nM, and 1 μ M), LY294002 (100 nM, 1 and 10 μ M), AktVIII
557 (100 nM, 1 and 10 μ M), Go6983 (10, 100 nM and 1 μ M), AZD6244 (10, 100 nM, and 1
558 μ M), SB203580 (100 nM, 1 and 10 μ M), or SB216763 (100 nM, 1 and 10 μ M)] for 10
559 min and then in the additional absence or presence of 100 nM insulin for 20 min, after
560 which cell extracts were subjected to SDS-PAGE with or without Phos-tag followed by
561 immunoblot analysis with antibodies to the indicated proteins. Phosphorylation of
562 ERK1/2 and MAPKAPK-2 was examined to monitor inhibition of MEK (AZD6244)
563 and p38 mitogen-activated protein kinase (SB203580), respectively. (C) Serum-
564 deprived 3T3-L1 cells expressing GSK3 α , GSK3 β , or control shRNAs were incubated
565 with Torin1 (100 nM) or CHIR99021 (1 μ M) for 10 min and then in the additional
566 absence or presence of 100 nM insulin for 25 min, after which cell extracts were
567 subjected to analysis as in (A) and (B). (D) Immunofluorescence analysis of GSK3
568 (green) in serum-deprived 3T3-L1 cells incubated with or without 10 nM rapamycin or
569 100 nM Torin 1 for 1 h and then in the additional absence or presence of 100 nM insulin
570 for 30 min. Nuclei were stained with DAPI (blue). Scale bars, 20 μ m.

571

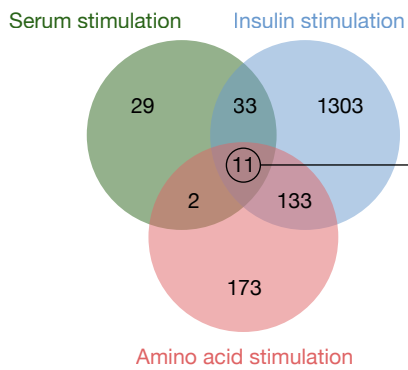
572 **Fig. 5. PP1 dephosphorylates PBX2 at Ser³³⁰.** (A) Serum-deprived 3T3-L1 cells were
573 incubated with calyculin A (0, 5, 10 or 50 nM) for 10 min and then in the additional
574 absence or presence of 100 nM insulin for 20 min, after which cell extracts were
575 subjected to SDS-PAGE with or without Phos-tag followed by immunoblot analysis
576 with antibodies to the indicated proteins. (B) Serum-deprived HeLa cells that had been
577 transfected with a control siRNA or siRNAs specific for the catalytic subunits of PP1 or
578 PP2A were stimulated with 100 nM insulin for 20 min, after which cell extracts were
579 analyzed as in (A). (C) Quantification of the Ser³³⁰-phosphorylated/Ser³³⁰-

580 dephosphorylated band intensity ratio for PBX2 relative to that of siControl cells for
581 immunoblots as in (B). Data are means \pm SEM from three independent experiments. **P*
582 < 0.05 , ***P* < 0.01 (Dunnett's test). (D) Immunocytofluorescence analysis of PP1
583 (green) in serum-deprived 3T3-L1 cells incubated with or without 10 nM rapamycin or
584 100 nM Torin 1 for 1 h and in the additional absence or presence of 100 nM insulin for
585 30 min. Nuclei were stained with DAPI (blue). Scale bars, 20 μ m.

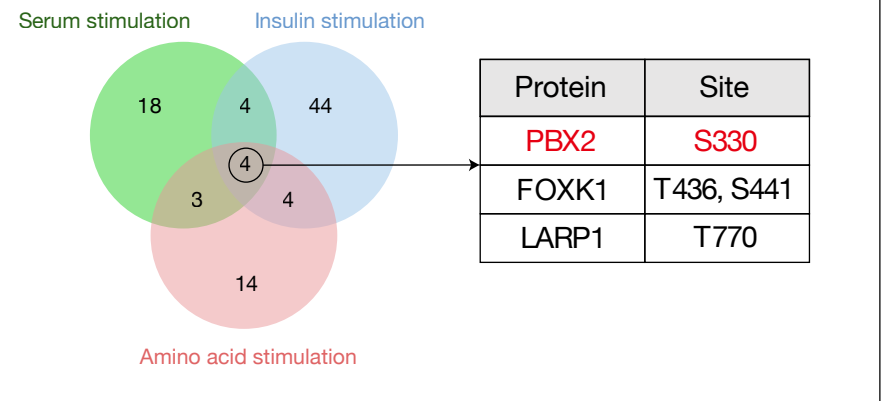


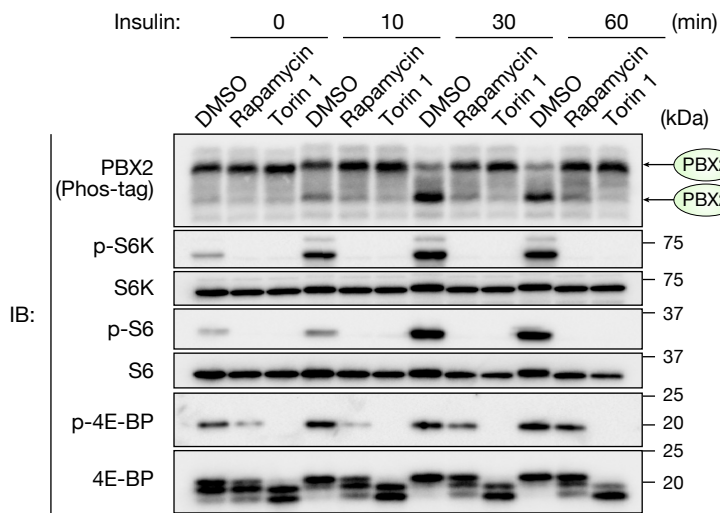
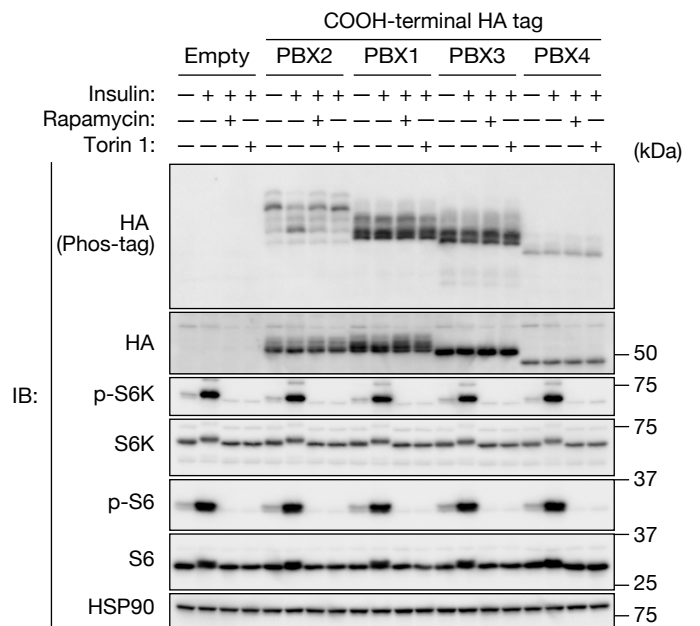
A**B**

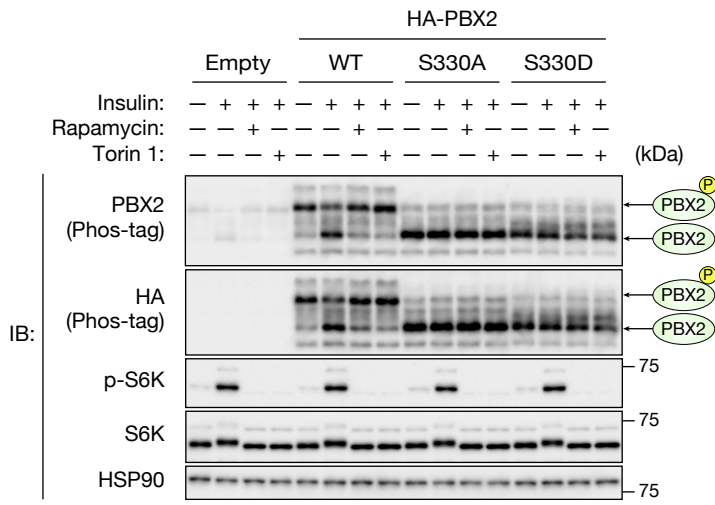
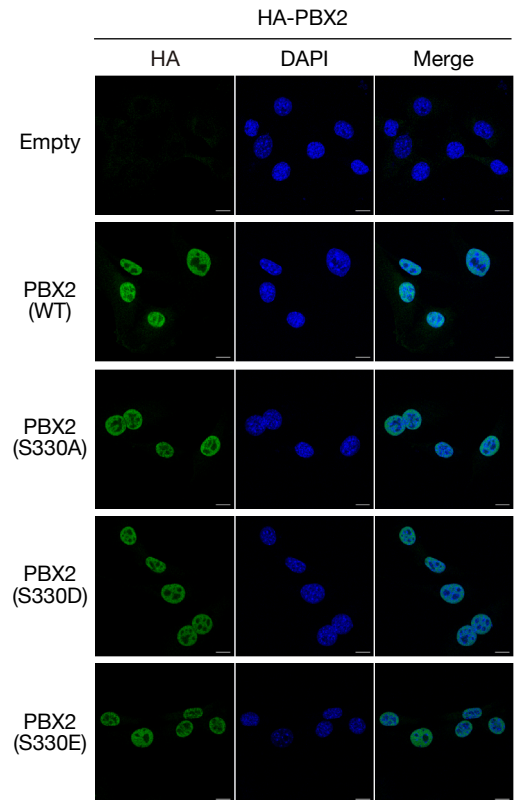
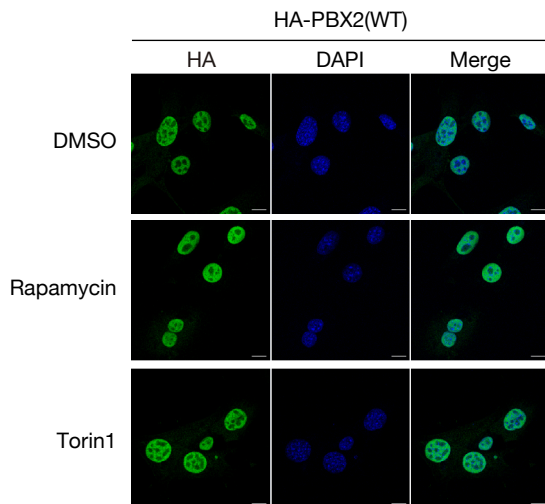
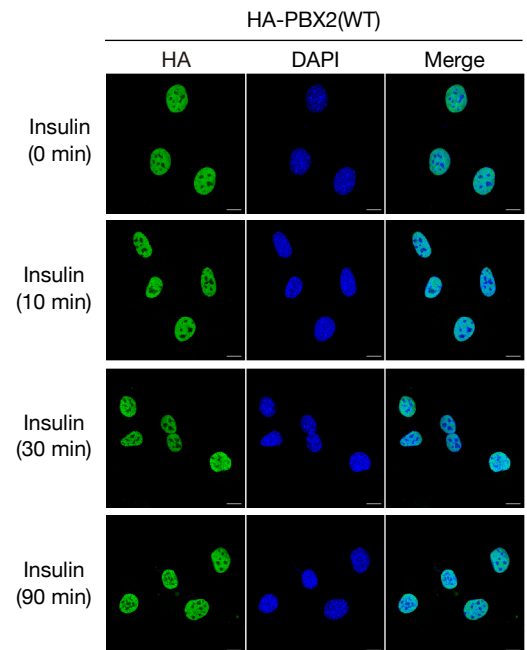
1684 dephosphorylated proteins

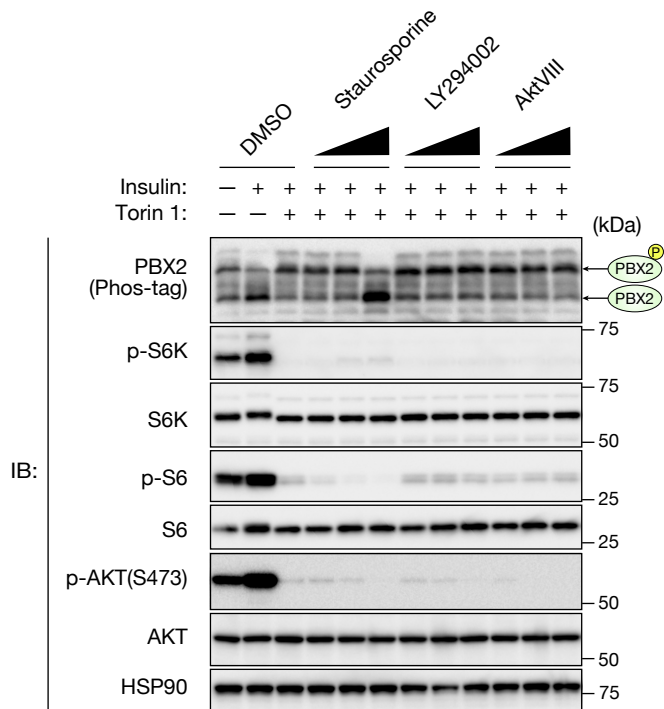
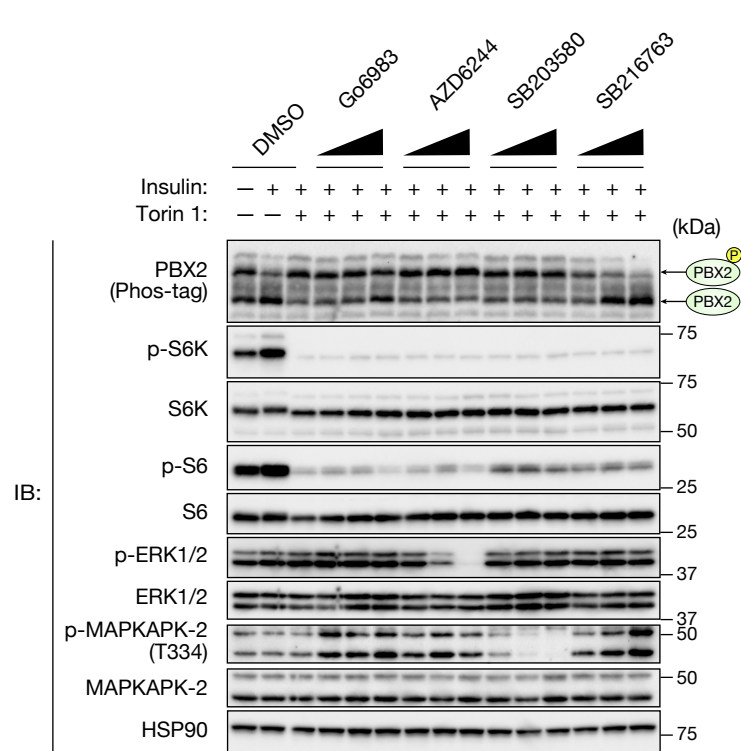
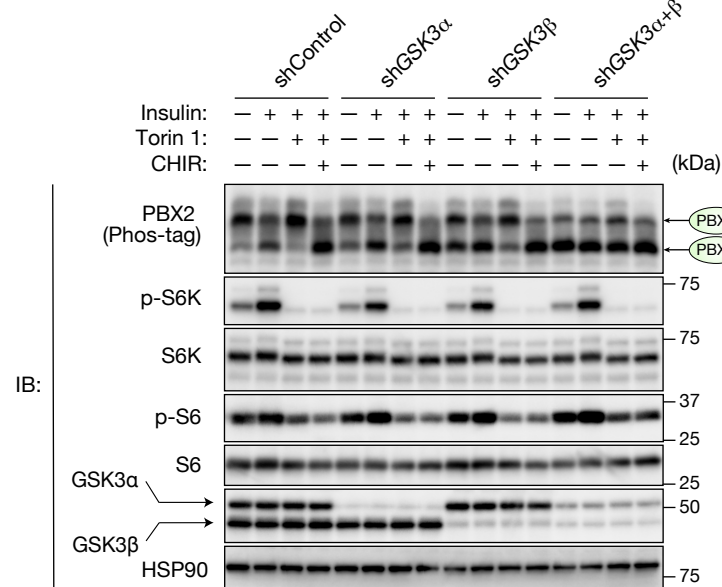
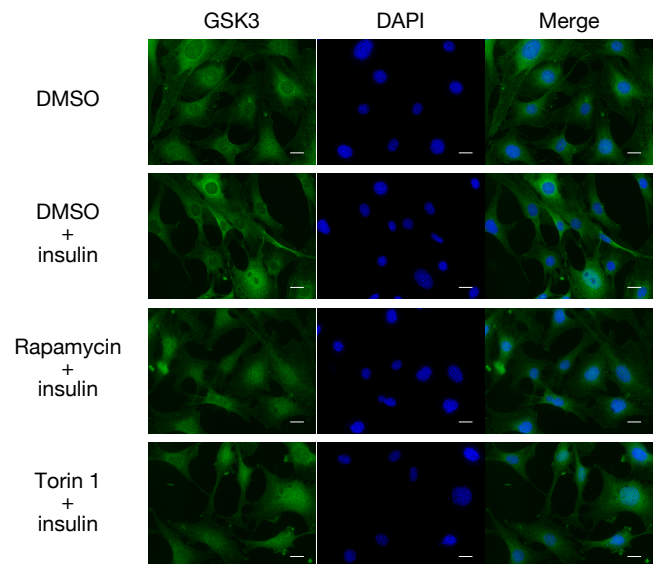


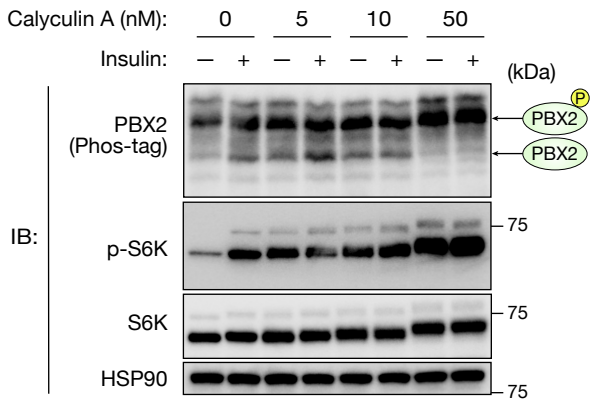
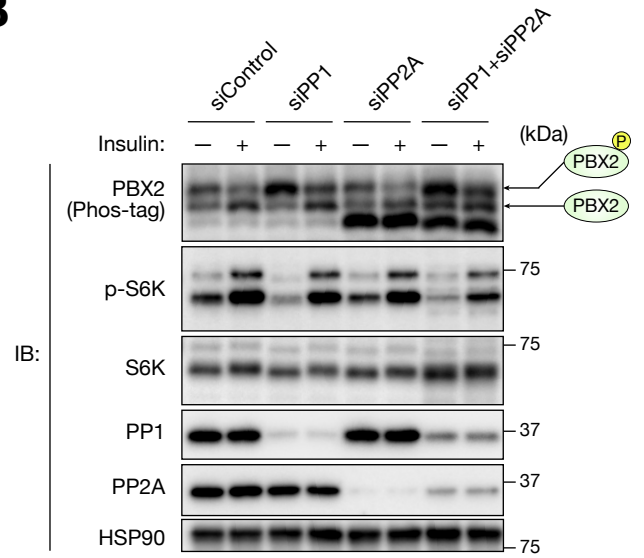
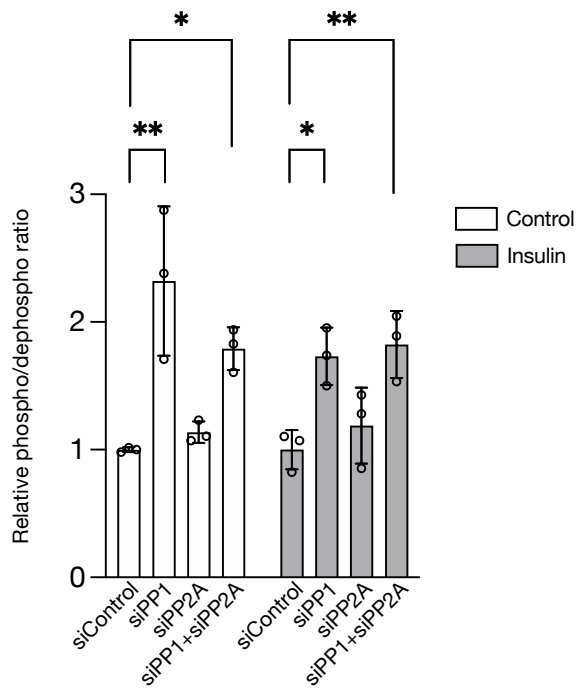
91 dephosphorylated sites of 11 dephosphorylated proteins



A**B**

A**B****C****D**

A**B****C****D**

A**B****C****D**